A Multi-target Tracking Algorithm for Application to Adaptive Cruise Control

Il-ki Moon
Department of Automotive Engineering, Hanyang University
Seoul 133-791, Korea
Kyongsu Yi*
School of Mechanical Engineering, Hanyang University,
Seoul 133-791, Korea
Derek Caveney, J. Karl Hedrick
Department of Mechanical Engineering, University of California,
Berkeley, Berkeley, CA, USA 94720

This paper presents a Multiple Target Tracking (MTT) Adaptive Cruise Control (ACC) system which consists of three parts; a multi-model-based multi-target state estimator, a primary vehicular target determination algorithm, and a single-target adaptive cruise control algorithm. Three motion models, which are validated using simulated and experimental data, are adopted to distinguish large lateral motions from longitudinally excited motions. The improvement in the state estimation performance when using three models is verified in target tracking simulations. However, the performance and safety benefits of a multi-model-based MTT-ACC system is investigated via simulations using real driving radar sensor data. The MTT-ACC system is tested under lane changing situations to examine how much the system performance is improved when multiple models are incorporated. Simulation results show system response that is more realistic and reflective of actual human driving behavior.

Key Words: Interacting Multiple Model, Probabilistic Data Association, Adaptive Cruise Control, Stop and Go Cruise Control, Advanced Safety Vehicle, Milli-meter Wave Radar

Nomenclature

$\mathbf{F}_j$: Transition matrix
g : Threshold
$\mathbf{H}_j$: Measurement matrix
R : Covariance matrix of measurement noise
r : Radius of polar coordinate
$\mathbf{P}_i[k-1]$: Filtered covariance matrix
$Q_j[k]$: Covariance matrix of process noise
$\hat{\mathbf{x}}[k-1]$: State estimate
$\hat{\mathbf{x}}_i[k-1]$: Filtered estimate of the state vector
z_1 : Longitudinal distance of Cartesian coordinate
z_2 : Lateral distance of Cartesian coordinate
$\hat{\mathbf{z}}_j[k|k-1]$: Predicted measurement
α_1 : Rejection the correct radar return
α_2 : Probability that the correct return will not be detected
$\boldsymbol{\Gamma}_j$: Input distribution matrix
θ : Angle of polar coordinate
σ_r : Longitudinal Standard deviation of measurement error in polar coordinate
σ_θ : Lateral Standard deviation of measurement error in polar coordinate
$\mu_i[k-1]$: Updated mode probability
π : Markovian transition probability
$\chi_i[k]$: Event; ith validated measurement

* Corresponding Author,
E-mail : kyongsu@hanyang.ac.kr
TEL : +82-2-2220-0455; **FAX** : +82-2-2296-0561
School of Mechanical Engineering, Hanyang University, Seoul 133-791, Korea. (Manuscript **Received** March 14, 2005; **Revised** July 30, 2005)

1. Introduction

In recent years, Advanced Vehicle Safety Systems (AVSS) have been an interesting and active research topic. Adaptive Cruise Control (ACC) (Shladover et al., 1991; Hedrick et al., 1994; Peng, 1998; Venhovens, 2000; Yi et al., 2001; 2002) systems, one field of AVSS, have goals that include the partial automation of longitudinal vehicle control and the reduction of the driver's workload. First generation ACC systems have been commercialized by many major automotive manufacturers. In practical driving situations, although there are several vehicles in front of the subject vehicle, each driver is following just one car, the target vehicle, which is in the same lane or is cutting-in from a neighboring lane. The driver's decision of which vehicle is the target vehicle is a complicated one, but established ACC algorithms use simple schemes which declare the target vehicle as the closest one currently in my lane. One goal of this paper is to present a more intelligent decision process which incorporates the tracking of multiple preceding vehicles simultaneously.

A sensor for preceding object detection is the most important component to an ACC system because it directly influences the performance of the system. Milli-meter Wave (mmW) radar (Tokoro, 1996) is a preferred technology because the influence of environmental conditions, like rain and fog, is smaller than that of other ranging technologies like ultra-sonar, laser, and vision. With the measurements available from a ranging sensor, the Kalman filter is the preferred state estimator in a target tracking algorithm. However, its single model dynamics cannot accurately describe all possible target motions. The Interacting Multiple Model (IMM), which was introduced by Blom (Blom et al., 1984) and further developed by Bar-Shalom (Bar-Shalom, 1978; Bar-Shalom and Fortmann, 1988) has a finite number of Kalman filters that each describe the characteristics of a particular target motion. With this finite bank of filters, it is desired that at all times, there will be one model that accurately reflects the current motion of the target.

Unfortunately, ranging sensors are rarely operated in environments devoid of false detections or clutter. In recent decades, several algorithms were developed for tracking a moving target in such clutter and the Probabilistic Data Association Filter (PDAF) introduced by Bar-Shalom and Tse (1975) showed superior performance. Bar-Shalom (Li and Bar-Shalom, 1993) combined these two algorithms, the IMM and the PDAF, into a practical aerospace target tracking routine because of their common use of probability theory and their complementary nature in terms of common variables. Caveney (Caveney and Hedrick, 2002) contributed to the evaluation of Bar-Shalom's IMM-PDAF algorithm as an automotive target tracking routine via vehicle tests. However, previous IMM-PDAF research in vehicular applications has been based on two motion models; one is a uniform motion model where acceleration variation is small and the other is a maneuvering motion model where acceleration variation can be large.

In this paper, we present three motion models that separate lateral movement from longitudinal motion in previous maneuvering motion models. This allows lane changes to be distinguished from braking maneuvers. The probability of a lane change motion model is used as an additional input to the controller which determines which track is the target vehicle. We apply the IMM-PDAF tracking routine, based on these three motion models (uniform motion, lane change, and braking), to an ACC simulation model and verify our adaptive controller under several critical driving situations. In particular, the MTT-ACC system is tested under severe braking situations and lane changing situations to examine how much the system performance is improved when multiple models are incorporated.

2. MTT-ACC Simulation Model

This section describes both the motion models of the IMM algorithm as a target state estimator and the primary target determination algorithm for the MTT-ACC simulation. The equations of

the IMM-PDAF routine are shown in the Appendix. The ACC system model in (Yi et al., 2001 ; 2002) is used in the closed-loop simulations of the MTT-ACC system. It and others are assumed to be known well enough that their equations are not repeated in this paper.

2.1 The three dynamic motion models

The motions of target vehicles are described by the following discrete-time, state-space models,

$$\begin{aligned}\mathbf{x}[k] &= \mathbf{F}\mathbf{x}[k-1] + \boldsymbol{\Gamma}\mathbf{w}[k-1] \\ &= [x\ \dot{x}\ y]^T\end{aligned} \tag{1}$$

where $\mathbf{x}[k]$ is a state vector in the horizontal Cartesian plane, x is the target's relative longitudinal position, $\dot{x}$ is the relative longitudinal velocity, y is the relative lateral position, and $\mathbf{w}[k]$ is white process noise assumed to be Gaussian distributed with zero mean and known covariance, $\mathbf{Q}[k]$. All three discrete-time, state-space models have the following transition matrix, $\mathbf{F}$, and the input distribution matrix, $\boldsymbol{\Gamma}$,

$$\mathbf{F}=\begin{bmatrix}1 & T & 0\\ 0 & 1 & 0\\ 0 & 0 & 1\end{bmatrix},\ \boldsymbol{\Gamma}=\begin{bmatrix}T & 0\\ 1 & 0\\ 0 & 1\end{bmatrix} \tag{2}$$

where T is the sampling time, taken as 0.05 sec in this paper.

Because the process noise term of second order dynamic motion model is speed variation and that of third order dynamic motion model is acceleration variation, the probability of lane-change motion cannot sufficiently excited while a preceding vehicle has a constant lateral velocity. Therefore, 2nd order longitudinal dynamics and 1st order lateral dynamics are chosen in this study.

The measurement model described in Equation (3) shows that only the longitudinal and lateral relative positions of each target are measured, although mmW radar can also transmit relative speeds of preceding vehicles.

$$\mathbf{z}[k]=\mathbf{H}\mathbf{x}[k]+\mathbf{v}[k] \tag{3}$$

$$\mathbf{H}=\begin{bmatrix}1 & 0 & 0\\ 0 & 0 & 1\end{bmatrix} \tag{4}$$

where $\mathbf{v}[k]$ is also a white, Gaussian, noise sequence with zero-mean and associated covariance, $\mathbf{R}[k]$.

All motion models use Equations (1)-(4), and only differ in their chosen process noise covariance matrices, $\mathbf{Q}[k]$, which reflect different perturbations of longitudinal vehicle speed and lateral vehicle position.

$$\mathbf{Q}=\boldsymbol{\Gamma}\begin{bmatrix}\sigma_{\nu x}^2 & 0\\ 0 & \sigma_{\omega y}^2\end{bmatrix}\boldsymbol{\Gamma}^T \tag{5}$$

where $\sigma_{\nu x}$ is the deviation of the vehicle's longitudinal speed and $\sigma_{\omega y}$ is the deviation of the vehicle's lateral position.

As mentioned earlier, for the vehicular application, we focus on early detection of and distinction between lateral motions and rapid decelerations. Past work has used only two motion models to detect any form of maneuver, namely, uniform motion and maneuvering motion. However, lateral deviations should be distinguished from longitudinally excited motions in the maneuvering motion model. Especially this knowledge will be used in the primary target determination algorithm. Thus, in this paper, we present three motion models which will be validated using simulated and experimental data in Section 2.2.

Our motion models are : uniform motion (Model 1) with ($\sigma_{\nu x}=1.1\times10^{-6}$[m/s], $\sigma_{\omega y}=1\times10^{-8}$[m]), lane-changing motion (Model 2) with ($\sigma_{\nu x}=1.23\times10^{-3}$[m/s], $\sigma_{\omega y}=9.8\times10^{-4}$[m]) and acceleration/deceleration motion (Model 3) with ($\sigma_{\nu x}=1.0\times10^{-1}$[m/s], $\sigma_{\omega y}=1.20\times10^{-7}$[m]). Although Model 3 represents both acceleration and deceleration motions, we will focus on its ability to model braking maneuvers and, therefore, refer to it as the braking motion model.

2.2 Validation of the three dynamic motion model set-up

In order to validate the proposed motion model set, we look at several simulations. Figure 1 depicts simulation results when the preceding vehicle and the subject vehicle have the same longitudinal speed. In this case, the uniform motion model should be the dominant motion model, as

measured by the model probabilities, because there is no relative acceleration between the two vehicles. In Figure 1(a), the estimated values track exactly the actual target's position at a longitudinal distance of 120 m and a lateral distance of 8 m. Figure 1(b) shows that uniform motion becomes the dominant motion among the three motions, but the converged probability, 0.47, is very low compared to 0.84 when two motion models (See Figure 1(c)) are employed using the parameters in the paper of Caveney (Li and Bar-Shalom, 1993). The steady state performance is influenced by the choice of the Markovian transition matrix whose components are apriori transition probabilities from one model to another and to itself. Figure 1 shows that if larger probabilities were employed in the diagonal components of the Markovian transition matrix, then higher converged values of the model probabilities can be expected.

Equation (6) is the Markovian transition matrix used in this paper.

$$\pi_{ij}=\begin{bmatrix} 0.95 & 0.025 & 0.025 \\ 0.025 & 0.95 & 0.025 \\ 0.025 & 0.025 & 0.95 \end{bmatrix} \tag{6}$$

The purpose of this next simulation is to examine the suitability of the proposed lateral motion model in a lane-change situation. Figure 2 (a) and (b) display a comparison between the estimated track position and the actual preceding vehicle position measurements fed to IMM-PDAF routine. It can be seen that the estimated longitudinal and lateral positions track the preceding vehicle well. The lateral motion of the preceding vehicle begins at 16 sec and continues for 15 sec. Figure 2(c) shows through the model probabilities how the lane-change motion becomes the dominant motion at that time.

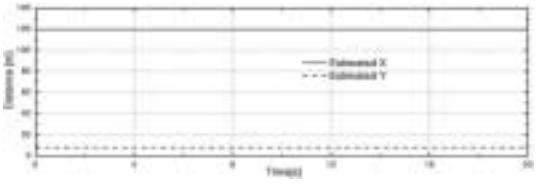

(a) Estimated position

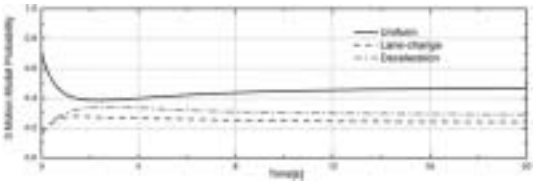

(b) Probabilities of the three motion models with 0.95 Markovian self-transition probability

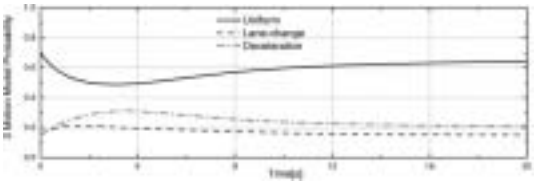

(c) Probabilities of three motion models with 0.98 Markovian self-transition probability

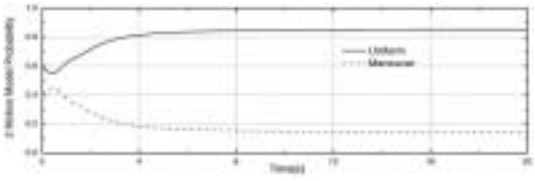

(d) Probabilities when only two motion models used

Fig. 1 Target state estimation of a vehicle with zero relative motion

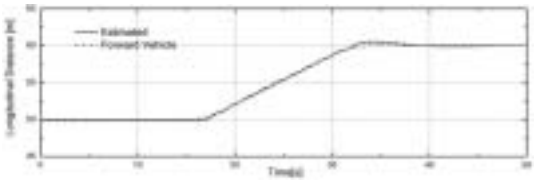

(a) Longitudinal position

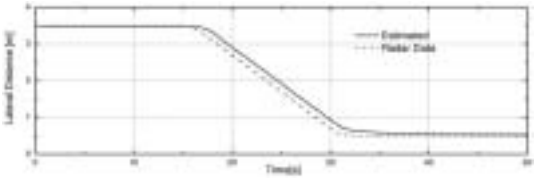

(b) Lateral position

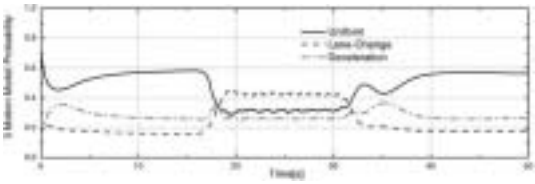

(c) Probabilities of the three motion models

Fig. 2 Target state estimation of a vehicle performing a lane change

Figure 3 shows the target tracking simulation results using experimental data acquired from a mmW radar on a middle-speed highway. Figure 3(a) and 3(b) display a comparison between the estimated track position and raw data from the mmW radar and they show good performance when three models are used. Figure 3(a) shows the longitudinal spacing between the preceding vehicle and the subject vehicle decreasing during the 4 sec and 9 sec mark and, subsequently, the probability of the braking motion model increasing at the same time. At about 5 sec, braking motion has become the dominant motion.

2.3 The primary target determination algorithm

The information concerning estimated target positions from the IMM-PDAF routine cannot be fed directly to a single-target ACC algorithm because it is only able to follow one preceding vehicle. Thus, there is a need to determine which preceding vehicle is the primary vehicle to be followed. In our primary target determination algorithm, there are two assumptions ; one is that the subject vehicle is in the center of the lane and the other is that the lane width is known. This covers the fact that the subject vehicle has no information on the relative position of the subject vehicle with respect to its own lane.

Generally, human drivers make the decision to follow the closest of any vehicles currently in their lane and any vehicles currently cutting into their lane. Figure 4 shows the flow chart of the primary target determination algorithm introduced here to incorporate additional information available from the multiple model tracking routine. This additional information allows us to adapt our ACC system to new primary targets in a way that is more intelligent and more reminiscent of human driving. Firstly, if the sign on the lateral position is opposite to that of the lateral speed, it means that the target is approaching the lane of the subject vehicle. When this occurs, a weighted lateral position is employed that is only used in this primary target decision process. This weight-

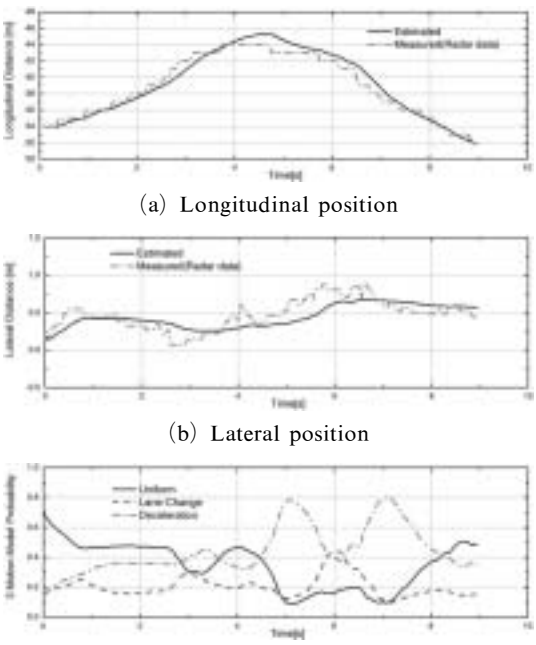

(a) Longitudinal position

(b) Lateral position

(c) Probabilities of three motion models

Fig. 3 Target state estimation of a rapidly braking vehicle

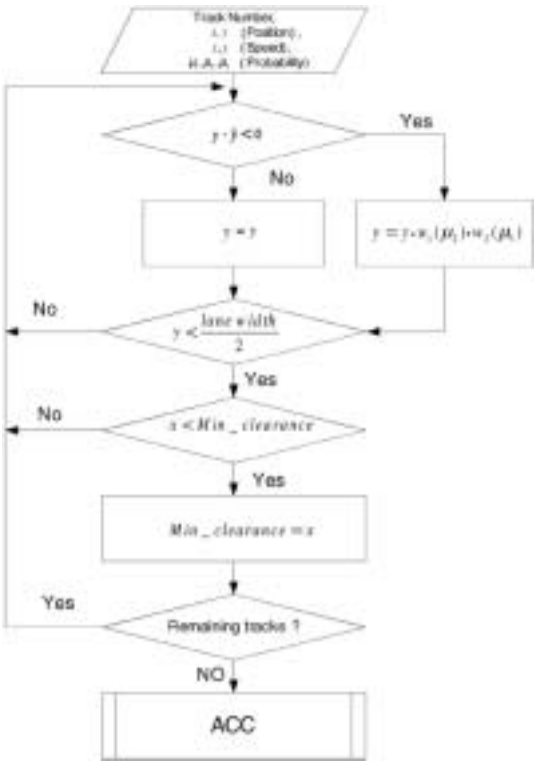

Fig. 4 Flow chart of the primary target determination algorithm

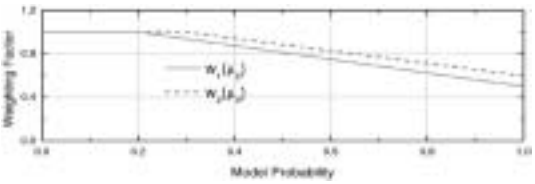

Fig. 5 Weighting factors enforced on the motion model probabilities

ing function makes a rapid decision possible while also considering the fact that the cut-in vehicle is not yet in the subject vehicle's lane.

The weighting factor functions, $w_1(\mu_2)$ and $w_2(\mu_3)$, introduced in Figure 4 are shown in Figure 5. The gradient of the weighting factor associated with the lane change motion model probability, $w_1(\mu_2)$, is steeper than that associated with the braking motion model probability, $w_2(\mu_3)$, because we focus on the predominant lateral motion exhibited during most lane changes. However, $w_2(\mu_3)$, exhibits the fact that acceleration and braking is also common during some lane changes.

3. Simulation Results

In this section, an MTT-ACC system that includes of the above multiple model tracker and primary target determination algorithm is tested via simulations using actual mmW radar data. However, the experimental radar data are related to the speed of the vehicle used to record the data. So, with the speed of the simulated subject vehicle being controlled by the ACC algorithm in a closed-loop simulation, we cannot use the mmW radar data directly. To overcome this drawback, we transform the raw data to a global frame of reference before running the simulations and calculate the relative measurements between surrounding vehicles and the subject vehicle as the simulation progresses.

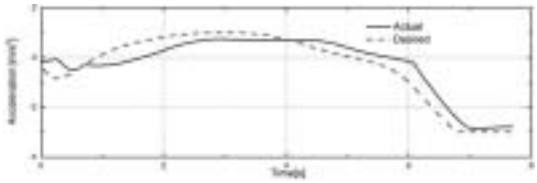

(a) Subject vehicle accelerations

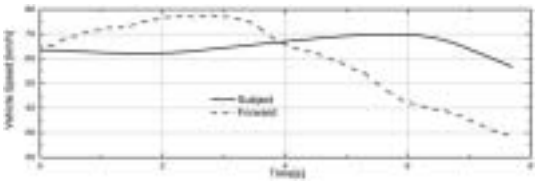

(b) Subject and forward vehicle speeds

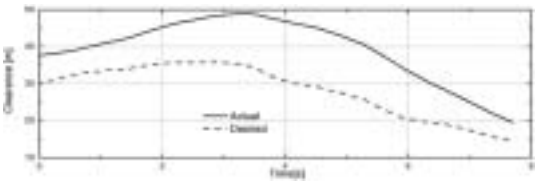

(c) Longitudinal position (Spacing)

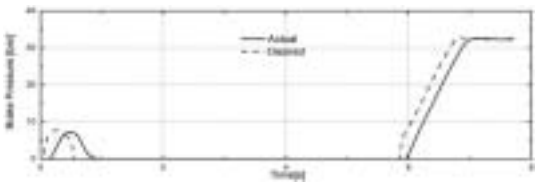

(d) Brake pressure

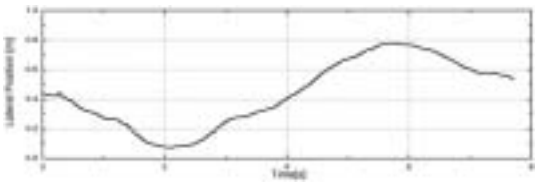

(e) Lateral position

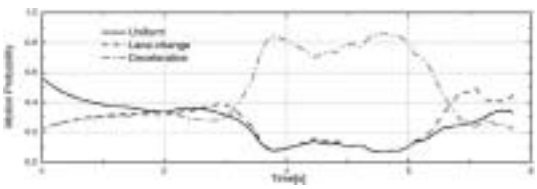

(f) Probability of three motion models

Fig. 6 ACC results in Deceleration Situation

3.1 Deceleration situation

Figure 6 shows the results of a simulation with a preceding vehicle braking. Subject and preceding vehicle accelerations and speeds are compared in Figure 6(a) and (b), respectively. It is illustrated that the subject vehicle tracks the deceleration of the preceding vehicle closely. Speed differences between the preceding vehicle and the subject vehicle are caused by the control

scheme which makes speed and spacing errors simultaneously converge to zero. Therefore, brake pressure is applied when the error between the desired and actual spacing becomes sufficiently small at 6 sec in Figure 6(d). The probability of the braking motion model has the largest value among the three motion models at 3.2 sec and then the lane change motion becomes a dominant motion at 6.5 sec in Figure 6(f).

3.2 Cut-in situation

Figure 7 shows vehicle trajectories plotted using real driving radar sensor data and estimated vehicle trajectories. Figure 7(a) shows a driving situation with a cut-in vehicle. The subject vehicle moves from (0 m, 0 m) to (0 m, 270 m) over the duration of this scenario. In this particular data run, most radar signals which have a negative lateral position can be discarded, because there was a median strip to the left of the center lane. The information of the cut-in vehicle is initially transmitted from data track 2 of the mmW radar and is later fed from data track 5 of the recorded data, beginning at 5.7 sec. Figure 7(b) shows the capabilities of the IMM-PDAF as a target state estimator. Most radar returns from clutter are removed and all targets, which move around the subject vehicle, are successfully tracked. Although the radar data of the cut-in vehicle jumps from data track 2 to data track 5, the estimated state of the cut-in vehicle is continuously fed from Track 2 of the IMM-PDAF routine. The preceding vehicle is in Track 1.

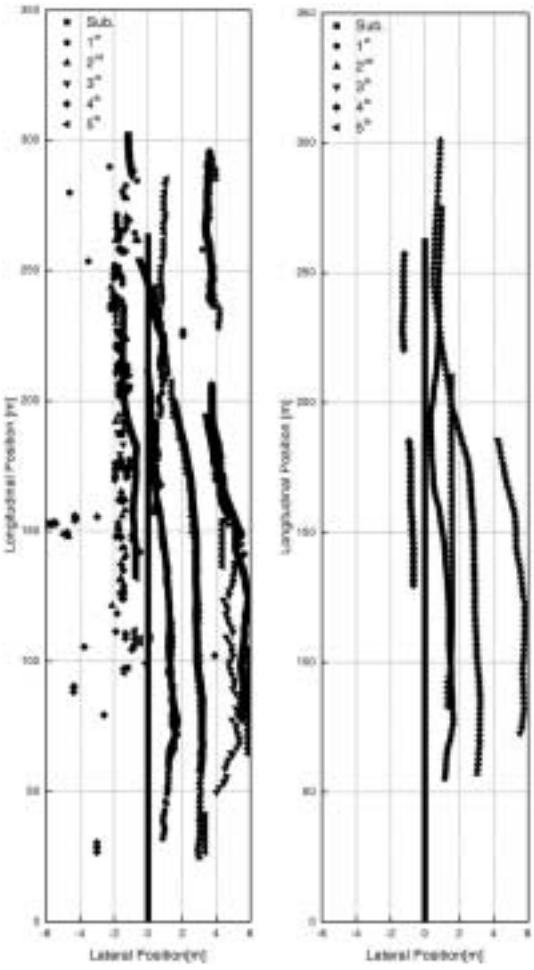

Fig. 7 MTT-ACC simulation results using driving data of a cut-in situation. (a) Data tracks from mmW radar (b) Estimated IMM-PDAF tracks

Figures 8 to 11 show the results of controlling the subject vehicle during the driving scenario of Figure 7. A time-gap of 1.57 sec and a minimum spacing of 2 m are used, which are estimated from investigating the data of the driver who was driving during this scenario.

Comparison of the longitudinal positions of Track 1 and Track 2 are shown in Figure 8(a). The lateral positions of Track 1 and Track 2 are compared in Figure 8(b). As shown in Figures 8(a) and 8(b), the cut-in vehicle in the right lane approaches the lane of the subject vehicle at 8 seconds and completely occupies the place in front of the subject vehicle at 11 seconds. The model probabilities of the cut-in vehicle are shown in Figure 8(c). The figure shows that the braking motion model probability increases at 6 sec, and then the lane change motion model probability rises rapidly. Most experimental data shows this phenomenon that the lane change is accompanied with a longitudinal acceleration or deceleration motion. In Figure 8(d), the subject vehicle has no target for one second because the IMM-PDAF routine requires time for initiation and confirmation of new target tracks. The controller of the ACC system recognizes the cut-in

vehicle as a primary target at about 8 sec in Figure 8(d). Moreover, this recognition by the probability-based method is two seconds faster than that of a simple method using only the lane width and lateral position of targets.

As a result of late recognition of the cut-in vehicle when using the simple method, the subject vehicle has a maximum vehicle speed of 70 km/h in Figure 9(a). Conversely, when using the probability-based primary target determination algorithm, the speed of the subject vehicle decreases starting at 8 sec and only has a maximum value of 66.7 km/h in Figure 9(b).

Furthermore, the distance between the subject and the cut-in vehicle, when the primary target is switched using the probability-based method at 8 sec, is around 23 m in Figure 10(b). However, the distance in Figure 10(a) when the primary target is switched at 10 sec using the simple method is about 17.3 m. Figure 10(a) shows that the subsequent minimum spacing using the simple method is 12.5 m at 12.1 sec, whereas the probability-based method results in a minimum spacing of 17.9 m at 10.1 sec in Figure 10(b).

The resulting control using the probability-based method and the simple method are compared in Figure 11. Figure 11(a) shows that the

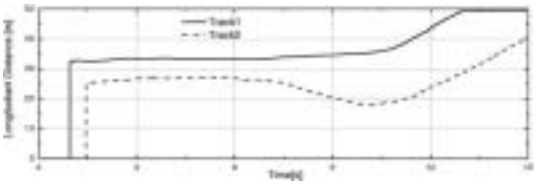

(a) Longitudinal position (Probability-based method)

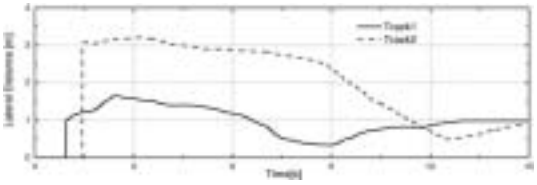

(b) Lateral position (Probability-based method)

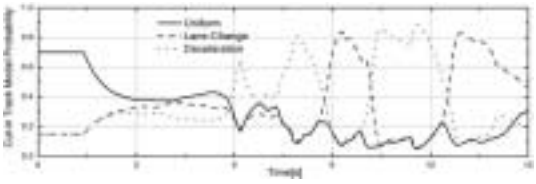

(c) Probability of three motion models (Probability-based method)

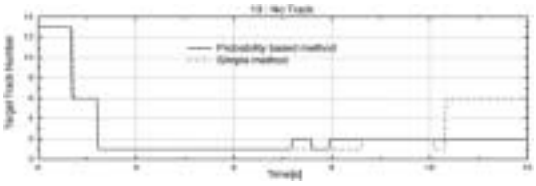

(d) Primary target number

Fig. 8 ACC results using simple method versus probability-based method (Lane-change situation)

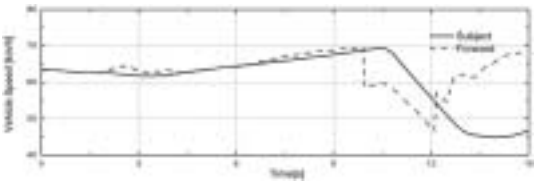

(a) Vehicle speed (Simple method)

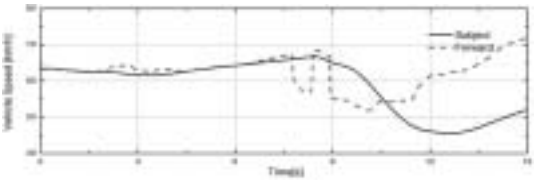

(b) Vehicle speed (Probability-based method)

Fig. 9 Vehicle speed using simple method versus probability-based method (Lane-change situation)

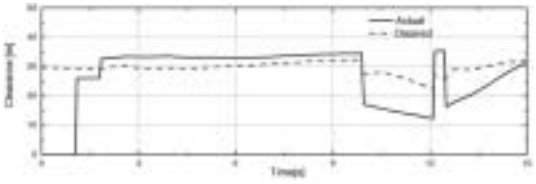

(a) Spacing (Simple method)

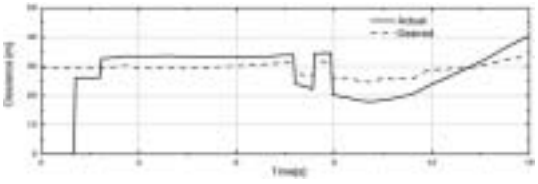

(b) Spacing (Probability-based method)

Fig. 10 Spacing: simple method versus probability-based method (Lane-change situation)

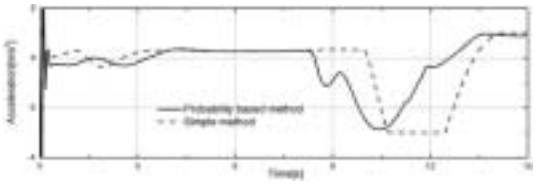

(a) Acceleration

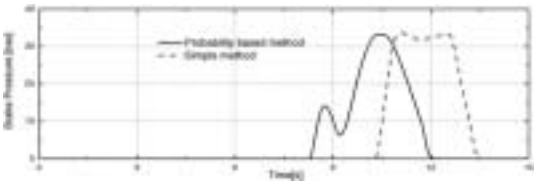

(b) Brake pressure

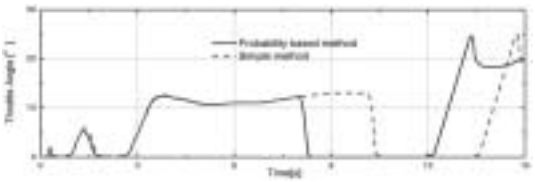

(c) Throttle angle

Fig. 11 Control results : simple method versus probability-based method (Lane-change situation)

faster recognition of the cut-in vehicle makes it possible for more comfortable driving. The ACC controller activates the brakes earlier to avoid a collision between the subject vehicle and the cut-in vehicle. A brake pressure of about 33 bar is applied at 10.5 sec in Figure 11(b).

4. Conclusions

A Multi-target tracking algorithm and its application to an Adaptive Cruise Control system have been presented. A multiple-model target state estimator which uses the IMM-PDAF algorithm consists of three motion models ; uniform motion, lane-change motion, and braking motion. Improvement in the target estimation performance using three motion models has shown through tracking simulations. A primary target determination algorithm that uses the motion model probabilities of the IMM-PDAF routine has been presented and the overall performance of the MTT-ACC algorithm has been investigated via closed-loop simulations using experimental data from a mmW radar. In the case of a cut-in situation, the primary target determination algorithm makes the ACC system switch primary targets earlier and subsequently provides additional clearance for the subject vehicle. Furthermore, this is a more realistic system response that better reflects actual human driving behavior.

Acknowledgments

This research has been supported by the NRL Project.

References

Bar-Shalom, Y., 1978, "Tracking Methods in a Multitarget Environment," *IEEE Transactions on Automatic Control*, Vol. AC-23, pp. 618~626.

Bar-Shalom, Y. and Fortmann, T. E., 1988, "Tracking and Data Association," *Academic Press*, New York, NY.

Bar-Shalom, Y. and Tse, E., 1975, "Tracking in a Cluttered Environment With Probablistic Data Association," *Automatica*, Vol. 11, pp. 451~460.

Blom, H. A. P. and Bar-Shalom, Y., 1984, "An Efficient Filter for Abruptly Changing Systems," *Proceedings of the 23rd IEEE Conference on Decision and Control*, pp. 656~658.

Caveney, D. and Hedrick, J. K., 2002, "Single versus Tandem Radar Sensor Target Tracking in the Adaptive Cruise Control Environment," *Proceedings of the 2002 American Control Conference*, Anchorage, Alaska.

Hedrick, J. K, Tomizuka, M. and Varaiya, P., 1994, "Control Issues in Automated Highway Systems," *IEEE Control Systems Magazine*, Vol. 14, No. 6, pp. 21~32.

Li, R. L. and Bar-Shalom, Y., 1993, "Design of an Interacting Multiple Model Algorithm for Air Traffic Control Tracking," *IEEE Transactions on Control System Technology*, Vol. 1, No. 3, pp. 186~194.

Peng, H., 1998, "Optimal Adaptive Cruise Control with Guaranteed String Stability," AVEC 98.

Shladover, S., et al., 1991, "Automated Vehicle Control Developments in the PATH Program," *IEEE Transactions on Vehicular Technology*, Vol. 40, No. 1, pp. 114~130.

Tokoro, S., 1996, "Automotive Application Systems of a Millimeter-wave Radar," *Proceedings of the 1996 IEEE Intelligent Vehicles Symposium*, pp. 260~265.

Venhovens, P., 2000, "Stop and Go Cruise Control," FISITA World Automotive Congress.

Yi, K., Hong, J. and Kwon, Y. D., 2001, "A Vehicle Control Algorithm for Stop-and-Go Cruise Control," *Proceedings of the Institution of Mechanical Engineers*, Part D, Vol. 215, No. 10, pp. 1099~1115.

Yi, K., Yoon, H. J., Huh, K., Cho, D., and Moon, I., 2002, "Implementation and Vehicle Tests of a Vehicle Stop-and-Go Cruise Control System," *Proceedings of the Institution of Mechanical Engineers*, Journal of Automobile Engineering, Vol. 216, Part D, pp. 537~544.

Appendix

Vehicle coordinates

Transformation from polar coordinates to Cartesian coordinates

$$z_1 = r\cos\theta,\ z_2 = r\sin\theta$$

Measurement errors are converted to Cartesian coordinates

$$\mathbf{R}[k] = \mathrm{cov}[\mathbf{v}[k]] \approx \frac{\sigma_r^2 - r\sigma_\theta^2}{2}\begin{bmatrix} b+\cos 2\theta & \sin 2\theta \\ \sin 2\theta & b-\cos 2\theta \end{bmatrix}$$

$$b = \frac{\sigma_r^2 + r^2\sigma_\theta^2}{\sigma_r^2 - r^2\sigma_\theta^2}$$

IMM (Interacting Multiple Model)

i, j : Motion model

r : The number of models

Mixing

Mixing probability

$$\mu_{i|j}[k-1] = \frac{\pi_{ij}\mu i[k-1]}{\sum_{i=1}^{r}\pi_{ij}\mu_i[k-1]}$$

Normalization factor

$$\bar{\mu}_j \triangleq \sum_{i=1}^{r}\pi_{ij}\mu_i[k-1]$$

Mixed initial condition of the state estimate

$$\hat{\mathbf{x}}_j^0[k-1] = \sum_{i=1}^{r}\hat{\mathbf{x}}_i[k-1]\mu_{i|j}[k-1]$$

Mixed initial condition covariance

$$\mathbf{P}_j^0[k-1] = \sum_{i=1}^{r}(\mathbf{P}_i[k-1] + [\hat{\mathbf{x}}_i[k-1] - \hat{\mathbf{x}}_j^0[k-1]] \times [\hat{\mathbf{x}}_i[k-1] - \hat{\mathbf{x}}_j^0[k-1]]^T)\mu_{i|j}[k-1]$$

Filtering

Predicted estimate of the state vector

$$\hat{\mathbf{x}}_j[k|k-1] = \mathbf{F}_j\hat{\mathbf{x}}_j^0[k-1] + \boldsymbol{\Gamma}_j\bar{\omega}_j[k-1]$$

Predicted covariance matrix of estimation errors

$$\mathbf{P}_j[k|k-1] = \mathbf{F}_j\mathbf{P}_j^0[k-1]\mathbf{F}_j^T + \boldsymbol{\Gamma}_j\mathbf{Q}_j[k]\boldsymbol{\Gamma}_j^T$$

Residual

$$\nu_j \triangleq \mathbf{z}[k] - \hat{\mathbf{z}}_j[k|k-1] = \mathbf{z}[k] - H_j\hat{\mathbf{x}}_j[k|k-1]$$

Covariance of the residual

$$\mathbf{S}_j[k] = \mathbf{H}_j\mathbf{P}_j[k|k-1]\mathbf{H}_j^T + \mathbf{R}_j[k]$$

Kalman filter gain

$$\mathbf{W}_j[k] = \mathbf{P}_j[k|k-1]\mathbf{H}_j^T\mathbf{S}_j[k]^{-1}$$

Filtered estimate of the state vector

$$\hat{\mathbf{x}}_j[k|k] = \hat{\mathbf{x}}_j[k|k-1] + \mathbf{W}_j[k]\nu_j$$

Filtered covariance matrix

$$\mathbf{P}_j[k|k] = \mathbf{P}_j[k|k-1] - \mathbf{W}_j[k]\mathbf{S}_j[k]\mathbf{W}_j[k]^T$$

Likelihood function

$$\Lambda_j[k] = |2\pi\mathbf{S}_j[k]|^{-1/2}e^{-\frac{1}{2}\nu_j^T[k]\mathbf{S}_j^{-1}[k]\nu_j[k]}$$

Updated model probability

$$\mu_j[k] = \frac{\Lambda_j[k]\bar{\mu}_j[k]}{\sum_{i=1}^{r}\Lambda_i[k]\bar{\mu}_i[k]}$$

Combination

State estimate

$$\hat{\mathbf{x}}[k]\hat{\mathbf{x}}[k|k] = \sum_{j=1}^{r}\hat{\mathbf{x}}[k|k]\mu_j[k]$$

Covariance matrix associated with state estimate

$$\mathbf{P}[k] \triangleq \mathbf{P}[k|k] = \sum_{j=1}^{r}(\mathbf{P}_i[k|k] + [\hat{\mathbf{x}}_j[k|k] - \hat{\mathbf{x}}[k|k]] \times [\hat{\mathbf{x}}_j[k|k] - \hat{\mathbf{x}}[k|k]]^T)\mu_j[k]$$

PDAF (Probabilistic Data Association Filter)

i : Validated measurement

k : Sampling time

$n[k]$: The number of validated measurements

j : Motion model

Set of validated measurements

$$Z[k]=\{\mathbf{z}_i[k]\}_{i=1}^{n[k]}$$

Cumulative set of measurements

$$Z^k=\{Z[l]\}_{l=1}^{k}$$

Residual

$$\begin{aligned}\nu_{j,i}[k]&\triangleq\mathbf{z}_i[k]-\hat{\mathbf{z}}_j[k|k-1]\\&=\mathbf{z}_i[k]-\mathbf{H}\hat{\mathbf{x}}_j[k|k-1]\end{aligned}$$

$$\{\mathbf{z}:\nu_{ji}[k]^T\mathbf{S}[k]^{-1}\nu_{j,i}[k]\leq g^2\}$$

Volume of validation region

$$V[k]=g^2\pi|\mathbf{S}[k]|^{1/2}$$

Probabilistic data association

$$\beta_{j,i}[k]\triangleq p(\chi_i[k]|Z^k)\quad i=0,\ 1,\ \cdots,\ n[k]$$

$$\sum_{i=0}^{nk}\beta_{j,i}[k]=1$$

$$\beta_{j,i}[k]=f_{j,k}(\mathbf{z}_i[k])\,[b[k]+\sum_{i=1}^{n[k]}f_{j,k}(\mathbf{z}_i[k])]^{-1}\quad i=1,\ \cdots,\ n[k]$$

$$\beta_{j,0}[k]=b[k][b[k]+\sum_{i=1}^{n[k]}f_{j,k}(\mathbf{z}_i[k])]^{-1}$$

$$f_{j,k}(\mathbf{z}_i[k])\triangleq(1-\alpha_1)^{-1}N(\nu_{j,i}[k]\,;0,\ S[k])$$

$$b[k]\triangleq n[k]\,V[k]^{-1}\frac{(\alpha_1+\alpha_2-\alpha_1\alpha_2)}{(1-\alpha_1)\,(1-\alpha_2)}$$

Kalman filter gain

$$\mathbf{W}_j[k]=\mathbf{P}_j[k|k-1]\mathbf{H}^T\mathbf{S}_j[k]^{-1}$$

State estimate for one model in an IMM

$$\begin{aligned}\hat{\mathbf{x}}_j[k|k]&=\sum_{i=0}^{n[k]}\beta_i[k]\hat{\mathbf{x}}_i[k|k]\\&=\hat{\mathbf{x}}_j[k|k-1]+\mathbf{W}_j[k]\nu_j[k]\end{aligned}$$

Combined residual

$$\nu_j[k]=\sum_{i=0}^{n[k]}\beta_{j,i}[k]\,\nu_{j,i}[k]$$

Covariance matrix associated with state estimate for one model in an IMM

$$\begin{aligned}\mathbf{P}_j[k|k]=&\beta_{j,0}[k]\mathbf{P}_j[k|k-1]+[1-\beta_{j,0}[k]]\mathbf{P}_j^0[k|k]\\&+\mathbf{W}_j[k][\sum_{i=0}^{n[k]}\beta_{j,i}[k]\,\nu_i[k]\,\nu_i[k]^T\\&-\nu[k]\,\nu[k]^T]\mathbf{W}_j[k]^T\end{aligned}$$

State estimate

$$\hat{\mathbf{x}}[k|k]=\sum_{j=1}^{r}\hat{\mathbf{x}}_j[k|k]\,\mu_j[k]$$

Covariance matrix associated with state estimate

$$\begin{aligned}\mathbf{P}[k|k]=&\sum_{j=1}^{r}(\mathbf{P}_j[k|k]+[\hat{\mathbf{x}}_j[k|k]-\hat{\mathbf{x}}[k|k]]\\&\times[\hat{\mathbf{x}}_j[k|k]-\hat{\mathbf{x}}[k|k]]^T)\,\mu_j[k]\end{aligned}$$